Phys. Fluids **18**, 051703 (2006).

A theoretical prediction of friction drag reduction in turbulent flow by superhydrophobic surfaces

Koji Fukagata, Nobuhide Kasagi

Department of Mechanical Engineering, The University of Tokyo,
Hongo 7-3-1, Bunkyo-ku, Tokyo 113-8656, Japan

Petros Koumoutsakos

Institute of Computational Science,
ETH Zürich, CH-8092, Switzerland

(Dated: 20 April 2006)

We present a theoretical prediction for the drag reduction rate achieved by superhydrophobic surfaces in a turbulent channel flow. The predicted drag reduction rate is in good agreement with results obtained from direct numerical simulations at $Re_\tau \simeq 180$ and 400. The present theory suggests that large drag reduction is possible also at Reynolds numbers of practical interest ($Re_\tau \sim 10^5 - 10^6$) by employing a hydrophobic surface, which induces a slip length on the order of ten wall units or more.

The prospect of using hydrophobic surfaces for drag reduction in practical applications (ranging from microfluidic devices to ship coatings) has attracted significant research efforts. The hydrophobicity of a surface is usually expressed in terms of a slip length, which quantifies the extent to which the fluid elements near the surface are affected by corrugations in the energy of the surface [1]. The slip length achieved by a chemical treatment of the surface is usually less than 1 μm [2], while combination of hydrophobic surface with micro/nano structure (*e.g.*, grooves [3], posts [4], particles [5], and turf [6, 7]) achieves slip length on the order of $10 - 100$ μm. It is usually postulated that large slip length is associated with large drag reduction.

Although intensive investigation has been made for laminar drag reduction, the effects induced by hydrophobic surfaces to turbulent flow had not been well understood until the very recent direct numerical simulation (DNS) performed by Min and Kim[8]. They considered turbulent channel flow at a constant flow rate. The friction Reynolds number of the no-slip flow was $Re_{\tau 0} = u_{\tau 0}\,\delta/\nu \simeq 180$ and the slip length considered was $l^{+0} \simeq 0.036 - 3.6$ (hereafter, the friction velocity of the no-slip flow and the corresponding wall unit are denoted by $u_{\tau 0}$ and the superscript of $+0$, whilst those in the slip flow are denoted by u_τ and the superscript of $+$, respectively.) Min and Kim[8] studied separately the effects of streamwise and spanwise slip as well as their combined effects. They reported that the streamwise slip decreases the drag, while the spanwise slip increases the drag. Through the examination of turbulence statistics and vorticity fields, they found the key physical mechanisms associated with drag increase/decrease.

The extension of DNS to high enough Reynolds numbers relevant for practical applications is beyond the capabilities afforded by today's computers. In order to complement simulations and experimental works, we derive in this Letter a formula which enables the prediction of drag reduction rate achieved with a given slip length under a wide range of Reynolds number. The present theory is based on the drag increase/decrease mechanisms proposed by Min and Kim[8]. The derivation of the formula is similar to that developed by Iwamoto *et al.*[10], for predicting theoretical drag reduction rate in the case of an idealized near-wall-layer damping. Throughout

TABLE I: Parameters in DNS of channel flow.

Re_b	$Re_{\tau 0}$	L_x	L_z	$N_x \times N_y \times N_z$	Δx^{+0}	Δy^{+0}_{max}	Δz^{+0}
5600	178	7δ	3.5δ	$128 \times 96 \times 128$	9.7	5.9	4.9
14000	394	6δ	3δ	$256 \times 192 \times 256$	9.2	6.4	4.6

this work, the term 'theory' is used for brevity to express the mathematical relationship obtained by using definitions of quantities, DNS data, and their implications.

We consider incompressible turbulent channel flow at a constant flow rate. Following Min and Kim [8], the hydrophobic wall boundary condition is modeled by slip velocities, *i.e.*,

$$u_s = l_x \left. \frac{\partial u}{\partial y} \right|_{wall} , \quad w_s = l_z \left. \frac{\partial w}{\partial y} \right|_{wall} . \tag{1}$$

Here, u_s and w_s denote the slip velocities in the streamwise and spanwise directions, respectively. The streamwise and spanwise slip lengths, l_x and l_z, are assumed constant. From a microscopic viewpoint, the slip length of a super-hydrophobic surface is not uniform in space. This non-uniformity may influence in a complex manner, as demonstrated by Ou and Rothstein [9]. However, if the size of each surface structure is much smaller than the Kolmogorov scale, the slip length in Eq. (1) may be regarded as a spatially averaged one in terms of turbulence dynamics. Therefore, the assumption of uniform slip length can be justified for nano-structured surface, such as NanoTurf [6, 7], in turbulent flow under practical conditions.

The drag reduction rate, R_D, is defined as

$$R_D = \frac{C_{f0} - C_f}{C_{f0}} = 1 - \left(\frac{u_\tau}{u_{\tau 0}} \right)^2 = 1 - \left(\frac{Re_\tau}{Re_{\tau 0}} \right)^2 , \tag{2}$$

where C_{f0} and C_f are the skin friction coefficients in no-slip and slip flows, respectively; Re_τ is the friction Reynolds number of the slip flow. From Eq. (2), the relationship between u_τ and $u_{\tau 0}$ is

$$u_\tau = \sqrt{1 - R_D}\, u_{\tau 0} , \tag{3}$$

or, can be expressed by the friction velocity of slip flow in the wall unit of no-slip flow:

$$u_\tau^{+0} = \sqrt{1 - R_D} . \tag{4}$$

Hence,

$$l_x^+ = u_\tau^{+0} l_x^{+0} , \quad l_z^+ = u_\tau^{+0} l_z^{+0} . \tag{5}$$

Prior to the presentation of theoretical results, which is the main objective of the Letter, we briefly introduce DNS performed in the present study. The DNS is used to develop and validate the present theory and serves also as a complement as well as independent verification of the previous study[8]. We consider larger slip length, $l_x^{+0} \simeq 3.6 - 180$ and $l_z^{+0} \simeq 3.6 - \infty$, at the bulk Reynolds number of $Re_b = 5600$ (*i.e.*, $Re_{\tau 0} \simeq 180$) as well as a higher Reynolds number, $Re_b = 14000$ (*i.e.*, $Re_{\tau 0} \simeq 400$), with $l_x^{+0} \simeq 0.4 - 400$ and $l_z^{+0} \simeq 0.4 - \infty$. The present DNS is performed using a second-order finite difference code, originally developed for pipe flow[11] and modified here to the Cartesian coordinates. The simulation parameters used in the present study are listed in Table I. These parameters are comparable to those used in related studies [8, 12, 13].

(a)

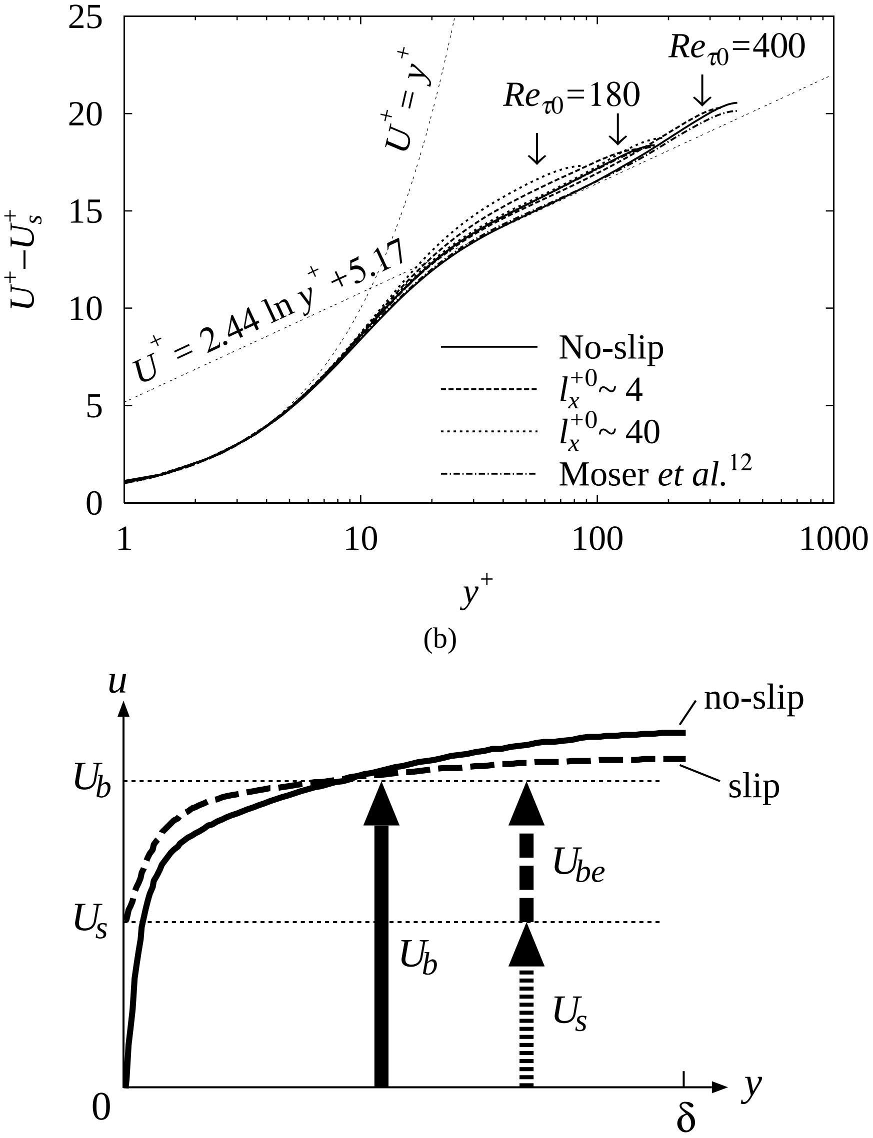

FIG. 1: Streamwise slip case: (a) mean velocity profile (keys of $l_x^{+0} \sim 4$ and 40 represent, respectively, $l_x^{+0} \simeq 3.6$ and 36 at $Re_{\tau 0} \simeq 180$, $l_x^{+0} \simeq 4.0$ and 40 at $Re_{\tau 0} \simeq 400$); (b) schematics of the drag decrease mechanism[8] and the effective bulk mean velocity, U_{be}.

First, we consider the streamwise slip only (*i.e.*, $l_z = 0$). In the wall units of slip flow, the mean slip velocity U_s is expressed as

$$U_s^+ = l_x^+ \left. \frac{dU^+}{dy^+} \right|_{wall} . \tag{6}$$

By definition, the mean wall-shear in the wall unit is always unity. Therefore, the relationship between U_s and l_x reads

$$U_s^+ = l_x^+ . \tag{7}$$

According to Min and Kim[8], the drag reduction in this case is mainly due to the direct effect of the mean slip velocity. As shown in Fig. 1(a), the mean velocity profile of the slip flow is

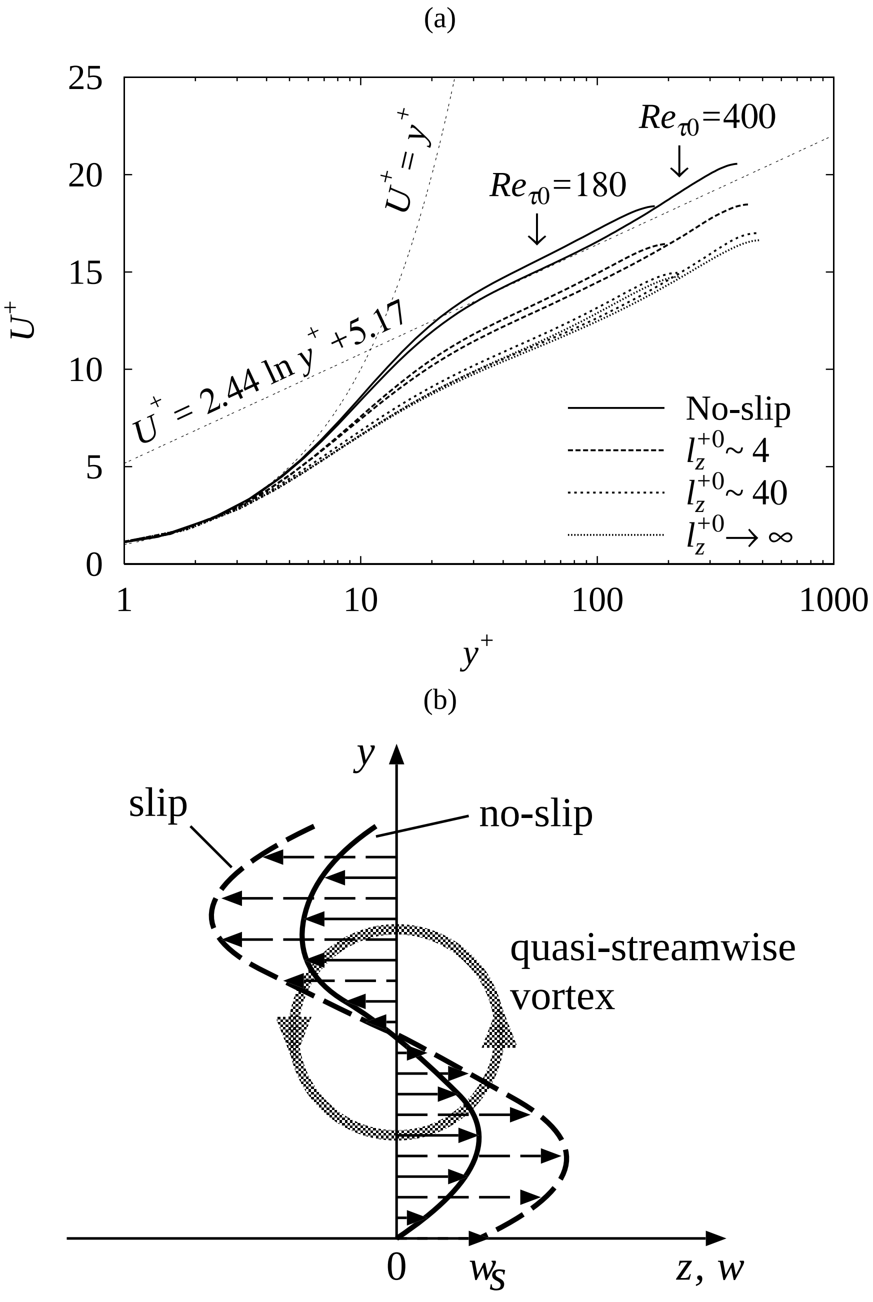

FIG. 2: Spanwise slip case: (a) mean velocity profile; (b) drag increase mechanism.[8]

nearly unchanged from the no-slip flow when they are scaled as $U^+ - U_s^+$, although deviation is noticeable when Re_τ becomes too low (*e.g.*, the case of $l_x^{+0} \simeq 36$ at $Re_{\tau 0} \simeq 180$, which results in $Re_\tau \simeq 88$). More specifically as illustrated in Fig. 1(b), the mean velocity profile of the slip flow, of which bulk mean velocity is U_b, can be considered as a summation of U_s and the profile of no-slip flow at a reduced (or, effective) bulk mean velocity, U_{be}:

$$U_b = U_s + U_{be} \ . \tag{8}$$

By using Eqs. (3)-(5) and (7), U_s can be expressed in terms of l_x^{+0} and $u_{\tau 0}$, as

$$U_s = (u_\tau^{+0})^2 \, l_x^{+0} u_{\tau 0} \ . \tag{9}$$

The bulk mean velocity of the no-slip flow can be expressed by using the log-law version of Dean's formula[14]:

$$U_b = \left(\frac{1}{\kappa}\ln Re_{\tau 0} + F\right) u_{\tau 0}\ , \tag{10}$$

where $\kappa = 0.41$ and $F = 3.2$ (corresponding to the log-law of $U^+ = 2.44\ln y^+ + 5.17$). As mentioned above, the mean velocity profiles scaled as $U^+ - U_s^+$ are nearly identical regardless of l_x. This observation suggests that Eq. (10) holds without modification also for the velocity profile of slip flow from which U_s^+ is subtracted. Therefore, by noting relationships (3) and (4), U_{be} can similarly be expressed as

$$U_{be} = \left[\frac{1}{\kappa}\ln\left(u_\tau^{+0} Re_{\tau 0}\right) + F\right] u_\tau^{+0} u_{\tau 0}\ . \tag{11}$$

Substitution of Eqs. (9)-(11) into Eq. (8) yields the relationship among $Re_{\tau 0}$, l_x^{+0} and u_τ^{+0}:

$$\frac{1}{\kappa}\ln Re_{\tau 0} + F = (u_\tau^{+0})^2\, l_x^{+0} + \left[\frac{1}{\kappa}\ln\left(u_\tau^{+0} Re_{\tau 0}\right) + F\right] u_\tau^{+0}\ , \tag{12}$$

or, by isolating l_x^{+0}:

$$l_x^{+0} = \frac{1 - u_\tau^{+0}}{(u_\tau^{+0})^2}\left(\frac{1}{\kappa}\ln Re_{\tau 0} + F\right) - \frac{1}{\kappa u_\tau^{+0}}\ln u_\tau^{+0}\ . \tag{13}$$

With the explicit formula (13), we can easily plot the relationship between l_x^{+0} and R_D $(= 1 - (u_\tau^{+0})^2$, see Eq. (4)) for given $Re_{\tau 0}$.

Next, we consider the spanwise slip wall only (*i.e.*, $l_x = 0$). As shown in Fig. 2(a), downward shift of the mean velocity profile occurs as the increase of l_z. This shift can be explained[8] by stronger motion of quasi-streamwise vortices, as shown in Fig. 2(b). Because this change occurs mostly in the region below the logarithmic layer, it would result in varying F in Eq. (10) while leaving κ unchanged. By the same reason, variation of F should not explicitly depend on the Reynolds number, but be scaled by the resulting friction velocity, u_τ. Namely, F should be a function of l_z^+ only. This hypothesis may be justified by the fact that F is, in practice, constant in the no-slip case [14], which is a special case with $l_z = 0$. Thus, Eq. (10) is modified to read

$$U_b = \left(\frac{1}{\kappa}\ln Re_\tau + F(l_z^+)\right) u_\tau\ . \tag{14}$$

From Eqs. (10) and (14), the relationship on the drag reduction rate is obtained as

$$\frac{1}{\kappa}\ln Re_{\tau 0} + F_0 = \frac{u_\tau^{+0}}{\kappa}\ln(u_\tau^{+0} Re_{\tau 0}) + u_\tau^{+0} F(u_\tau^{+0}\, l_z^{+0})\ , \tag{15}$$

where $F_0 = F(0)$. Once the functional form of $F(l_z^+)$ is known, the drag increase by the spanwise slip can be predicted by Eq. (15).

In this work, we propose the following form of $F(l_z^+)$:

$$F(l_z^+) = F_\infty + (F_0 - F_\infty)\exp\left[-\left(l_z^+/a\right)^b\right]\ , \tag{16}$$

where $F_\infty = \lim_{l_z^+ \to \infty} F(l_z^+)$. The present DNS data give a value of $F_\infty = -0.8$ both at $Re_{\tau 0} = 180$ and 400. Figure 3 shows the curve with $a = 7$ and $b = 0.7$ fitted to the DNS data. Consistent

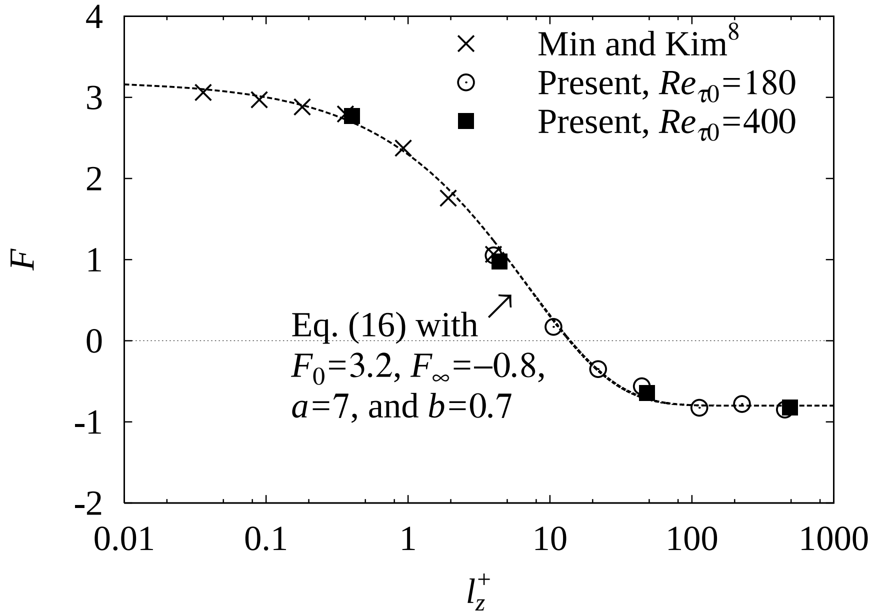

FIG. 3: Curve fit of $F(l_z^+)$.

with the hypothesis made above, there seems no significant Reynolds number effect on $F(l_z^+)$. Substitution of Eq. (16) into Eq. (15) yields an explicit formula:

$$l_z^{+0} = \frac{a}{u_\tau^{+0}} \left[-\ln\left\{ \frac{u_\tau^{+0}}{\kappa u_\tau^{+0}(F_0 - F_\infty)} \ln Re_{\tau 0} - \frac{\ln u_\tau^{+0}}{\kappa (F_0 - F_\infty)} + \frac{F_0 - u_\tau^{+0} F_\infty}{u_\tau^{+0}(F_0 - F_\infty)} \right\} \right]^{\frac{1}{b}} . \tag{17}$$

Finally, we consider slip both in the streamwise and spanwise directions. The sole assumption made here is that the driving mechanisms associated with the streamwise and spanwise slips act independently. Therefore, U_{be} in Eq. (8) is replaced by the right-hand-side of Eq. (15), and we obtain the unified formula:

$$\frac{1}{\kappa} \ln Re_{\tau 0} + F_0 = (1 - R_D)\, l_x^{+0} + \frac{\sqrt{1 - R_D}}{\kappa} \ln(\sqrt{1 - R_D}\, Re_{\tau 0}) + \sqrt{1 - R_D}\, F(\sqrt{1 - R_D}\, l_z^{+0}) . \tag{18}$$

In this case, an explicit formula like Eqs. (13) and (17) cannot be obtained. Nevertheless, R_D achieved with a given set of l_x^{+0}, l_z^{+0} and $Re_{\tau 0}$ can easily be found by a numerical computation.

Figure 4 shows the drag reduction rate predicted by using the proposed theoretical formula. In all cases, the theoretical predictions are in good agreement with the results of DNS for the whole range of slip length. There is an excellent agreement at $Re_{\tau 0} \simeq 400$, for which the low-Reynolds

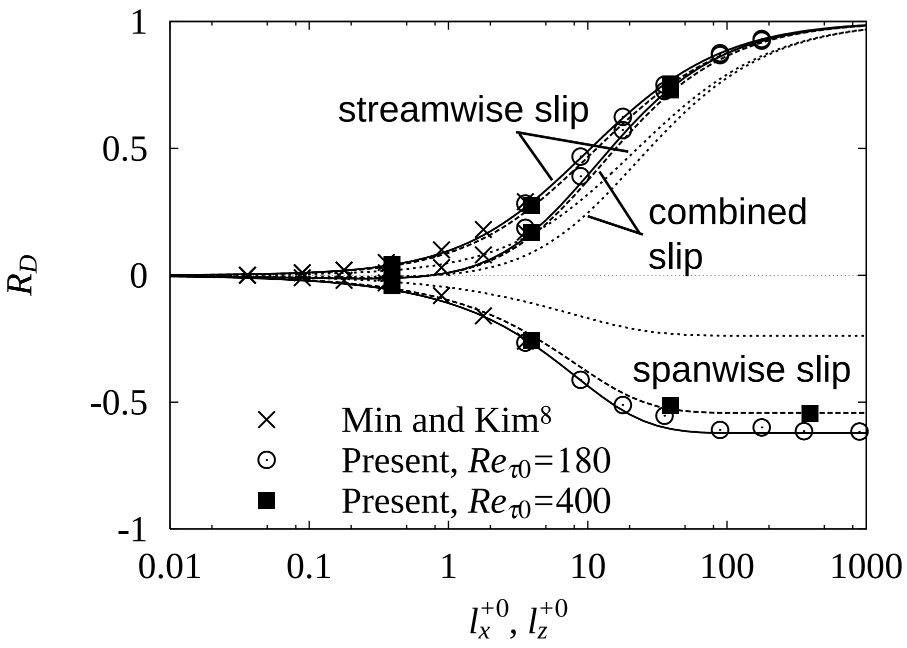

FIG. 4: Drag reduction rate, R_D, as a function of slip length. Symbols, DNS; lines, present theory (solid, $Re_{\tau 0} = 180$; dashed, $Re_{\tau 0} = 400$; dotted, $Re_{\tau 0} = 10^6$.)

number effect should be much weaker than $Re_{\tau 0} \simeq 180$. Moreover, the agreement in the combined slip case confirms the assumption additionally made for that case: the drag decrease and increase mechanisms by the streamwise and spanwise slips are independent each other. As the Reynolds number increases, the drag decrease effect by the the streamwise slip is gradually weakened, while the drag increase effect by the spanwise slip deteriorates faster. As a result, the Reynolds number dependency is also mild in the combined slip case.

As an application of the proposed formula, we estimate the drag reduction effect in a typical high-Reynolds-number application. The friction Reynolds number in the central part of a 300 m-class crude oil tanker running at 16 knot ($\simeq$ 8 m/s, a typical cruising condition) can be estimated as $Re_{\tau 0} \simeq 2 \times 10^5$. The friction velocity is $u_{\tau 0} \simeq 0.2$ m/s, resulting in one wall unit length to be about 5 μm. The boundary layer thickness is $\delta \simeq 0.8$m and the shear rate is $S \simeq 5 \times 10^4$ s^{-1}. The slip length of super-hydrophobic surfaces has not been measured under such a high shear rate. However, if we assume that the slip length remains at about 20 μm, which is the value of NanoTurf in water[7], $l_x^{+0} (= l_z^{+0})$ becomes about 4. The formula (18) predicts $R_D \simeq 10\%$ in this case. If the slip length can be improved to 50 μm (corresponding to NanoTurf in 30 wt% glycerin solution[7]) and $l_x^{+0} (= l_z^{+0})$ becomes 10, then the present theory implies considerable amount of drag reduction, $R_D \simeq 25\%$.

Acknowledgments

This work was supported through the 21st Century COE Program, “Mechanical Systems Innovation,” by the Ministry of Education, Culture, Sports, Science and Technology of Japan (MEXT). PK wishes to gratefully acknowledge the support of the 21st Century COE Program, during his sabbatical at the University of Tokyo.

[1] P. A. Thompson and S. M. Troian, "A general boundary condition for liquid flow at solid surfaces," Nature **389**, 360 (1997).

[2] C.-H. Choi, K. J. A. Westin, and K. S. Breuer, "Apparent slip flow in hydrophilic and hydrophobic microchannels," Phys. Fluids **15**, 2897 (2003).

[3] K. Watanabe, Yanuar, and H. Udagawa, "Drag reduction of Newtonian fluid in a circular pipe with a highly water-repellant wall," J. Fluid Mech. **381**, 225 (1999).

[4] J. Ou, B. Perot, and J. P. Rothstein, "Laminar drag reduction in microchannels using ultrahydrophobic surfaces," Phys. Fluids **16**, 4635 (2004).

[5] A. K. Balasubramanian, A. C. Miller, and O. K. Rediniotis, "Microstructured hydrophobic skin for hydrodynamic drag reduction," AIAA J. **42**, 411 (2004).

[6] J. Kim and C.-J. Kim, "Nanostructured surfaces for dramatic reduction of flow resistance in droplet-based microfluidics," in *Proc. IEEE MEMS 2002*, Las Vegas, 20-24 January 2002 (IEEE, 2002) p. 479.

[7] C.-J. Kim and C.-H. Choi, "Nano-engineered low-friction surface for liquid flow," in *Proc. 6th KSME-JSME Thermal and Fluids Engineering Conference*, 20-23 March 2005, Jeju, Korea (2005), Paper BB.01.

[8] T. Min and J. Kim, "Effects of hydrophobic surface on skin-friction drag," Phys. Fluids **16**, L55 (2004).

[9] J. Ou and J. P. Rothstein, "Direct velocity measurements of the flow past drag-reducing ultrahydrophobic surfaces," Phys. Fluids **17**, 103606 (2005).

[10] K. Iwamoto, K. Fukagata, N. Kasagi, and Y. Suzuki, "Friction drag reduction achievable by near-wall turbulence manipulation at high Reynolds numbers," Phys. Fluids **17**, 011702 (2005).

[11] K. Fukagata and N. Kasagi, "Highly energy-conservative finite difference method for the cylindrical coordinate system," J. Comput. Phys. **181**, 478 (2002).

[12] R. D. Moser, J. Kim, and N. N. Mansour, "Direct numerical simulation of turbulent channel flow up to $Re_\tau = 590$," Phys. Fluids **11**, 943 (1999).

[13] K. Iwamoto, Y. Suzuki, and N. Kasagi, "Reynolds number effect on wall turbulence: Toward effective feedback control," Int. J. Heat Fluid Flow **23**, 678 (2002).

[14] R. B. Dean, "Reynolds number dependence of skin friction and other bulk flow variables in two-dimensional rectangular duct flow," ASME Trans. J. Fluids Eng. **100**, 215 (1978).